Check for updates

# Adhesion of biofilm, surface characteristics, and mechanical properties of antimicrobial denture base resin

Ana Beatriz Vilela Teixeira[1], Mariana Lima da Costa Valente[1], João Pedro Nunes Sessa[1], Bruna Gubitoso[1], Marco Antonio Schiavon[2], Andréa Cândido dos Reis[1]*

[1]Ribeirão Preto School of Dentistry, University of São Paulo, Ribeirão Preto, Brazil
[2]Natural Sciences Department, Federal University of São João Del-Rei, São João Del-Rei, Brazil

**ORCID**
**Ana Beatriz Vilela Teixeira**
https://orcid.org/0000-0002-0679-0301

**Mariana Lima da Costa Valente**
https://orcid.org/0000-0002-8144-0467

**João Pedro Nunes Sessa**
https://orcid.org/0000-0002-4656-5408

**Bruna Gubitoso**
https://orcid.org/0000-0002-6674-9335

**Marco Antonio Schiavon**
https://orcid.org/0000-0002-1553-5388

**Andréa Cândido dos Reis**
https://orcid.org/0000-0002-2307-1720

**Corresponding author**
Andréa Cândido dos Reis
Ribeirão Preto School of Dentistry,
University of São Paulo, Av. do
Café, s/n, 14040-904, Ribeirão
Preto - SP, Brazil
**Tel** +551633150477
**E-mail** andreare73@yahoo.com.br

**PURPOSE.** This study incorporated the nanomaterial, nanostructured silver vanadate decorated with silver nanoparticles ($AgVO_3$), into heat-cured resin (HT) at concentrations of 2.5%, 5%, and 10% and compared the adhesion of multispecies biofilms, surface characteristics, and mechanical properties with conventional heat-cured (HT 0%) and printed resins. **MATERIALS AND METHODS.** $AgVO_3$ was incorporated in mass into HT powder. A denture base resin was used to obtain printed samples. Adhesion of a multispecies biofilm of *Candida albicans*, *Candida glabrata*, and *Streptococcus mutans* was evaluated by colony-forming units per milliliter (CFU/mL) and metabolic activity. Wettability, roughness, and scanning electron microscopy (SEM) were used to assess the physical characteristics of the surface. The mechanical properties of flexural strength and elastic modulus were tested. **RESULTS.** HT 10%-$AgVO_3$ showed efficacy against *S. mutans*; however, it favored *C. albicans* CFU/mL ($P < .05$). The printed resin showed a higher metabolically active biofilm than HT 0% ($P < .05$). There was no difference in wettability or roughness between groups ($P > .05$). Irregularities on the printed resin surface and pores in HT 5%-$AgVO_3$ were observed by SEM. HT 0% showed the highest flexural strength, and the resins incorporated with $AgVO_3$ had the highest elastic modulus ($P < .05$). **CONCLUSION.** The incorporation of 10% $AgVO_3$ into heat-cured resin provided antimicrobial activity against *S. mutans* in a multispecies biofilm did not affect the roughness or wettability but reduced flexural strength and increased elastic modulus. Printed resin showed higher irregularity, an active biofilm, and lower flexural strength and elastic modulus than heat-cured resin. [J Adv Prosthodont 2023;15:80-92]

## INTRODUCTION

Polymethylmethacrylate (PMMA) has been the most used material in removable prostheses manufacture for over 80 years.[1,2] One of the ways to obtain denture bases using PMMA is by packing and processing heat-cured resin or 3D printing. Heat-cured resin is the gold standard in denture fabrication; however, 3D printing produces complete dentures with greater precision in less time.[2,3]

In both techniques, PMMA shows inherent characteristics such as roughness and porosity, which favor biofilm accumulation.[1-3] Microbial adhesion in the denture base causes inflammation in the palate mucosa known as denture stomatitis, which affects 15% to 70% of denture wearers.[4] Denture stomatitis is characterized by an inflammatory disorder in the palate mucosa in contact with the denture base, is multifactorial in origin, and can be caused by trauma or fungal infections.[4-6] It is maintained by poor hygiene, continuous wear of dentures, diet, immunosuppression, and low salivary pH.[4,5-7]

*Candida spp.* is the main etiologic factor in denture stomatitis,[1,3,4,8] along with other species such as *Streptococcus spp.* that enhance its virulence.[4,9-11] This fungus is capable of adhering to the mucosa and the denture base, produces proteolytic enzymes that aid in tissue penetration, and changes from yeast to hyphal form.[12] Silver nanoparticle (AgNPs) solutions were demonstrated to reduce the formation and adherence of *Candida albicans*.[4]

The nanostructured silver vanadate decorated with silver nanoparticles (AgVO$_3$) is a nanomaterial composed of vanadium nanowires and AgNPs on its surface.[13] Its mechanism of action occurs through direct contact with fungal and bacterial cell membranes and ion release. Silver (Ag$^+$) and vanadium (V$^{5+}$) ions bind to SH-groups (thiols) on bacterial enzymes, disrupt metabolism and cellular replication, cause oxidative stress, and cell death.[13-15] The incorporation of AgVO$_3$ in dental materials demonstrated promising antimicrobial activity, including in PMMA, and can prevent microbial adhesion and denture stomatitis.[16-24]

Heat-cured and self-cured PMMA incorporated with AgVO$_3$ reduced the adhesion of monospecies biofilms of *Candida albicans*, *Streptococcus mutans*, *Staphy-lococcus aureus*, and *Pseudomonas aeruginosa*.[22,23] However, the efficacy of these materials against multispecies biofilm has not yet been evaluated. In multispecies biofilm the microbial interactions change, increasing the pathogenicity of *Candida spp.*, for example.[25] Surface roughness and wettability also directly influence the initial microbial adhesion since the smooth and hydrophilic surface makes *C. albicans* hyphal growth difficult.[4] When it comes to oral biofilms, these complex interactions between species must be reproduced to validate the action of an antimicrobial compound.

Thus, this study aimed to evaluate the adhesion of multispecies biofilm, surface characteristics, flexural strength, and elastic modulus of heat-cured resin incorporated with AgVO$_3$ compared to conventional heat-cured and printed resins. The null hypothesis was that AgVO$_3$ incorporation does not show antimicrobial action against multispecies biofilm and does not influence surface characteristics, flexural strength, or elastic modulus compared to heat-cured and printed resins.

## MATERIALS AND METHODS

Nanostructured silver vanadate decorated with silver nanoparticles (AgVO$_3$), first synthesized by Holtz *et al.*,[13] was obtained after a reaction between silver nitrate solution (99.8%; Merck KGaA, Darmstadt, Germany) and ammonium metavanadate solution (99%; Merck KGaA), each previously solubilized in 200 mL of distilled water at 65°C. The resulting solution was filtered and dried in a vacuum, obtaining the AgVO$_3$ powder.

The samples were prepared with 2.5, 5, and 10 wt% of AgVO$_3$ concentrations. The AgVO$_3$ powder was weighed on a precision scale, added and homogenized with a heat-cured resin (HT) powder (Classic Dental Articles, Sao Paulo, Brazil), and then manually mixed with liquid in a glass dappen dish with a lid. The material was packed and pressed into denture flasks containing molds of Ø9 × 2 mm and 65 mm × 10 mm × 3.3 mm. A group with conventional heat-cured resin (without the nanomaterial) was obtained (HT 0%). After the thermal polymerization cycle, the samples were polished in a grinding and polishing

machine with 80, 400, 600, and 1200 grit sandpapers.

Printed samples were obtained with Cosmos denture resin (Yller Biomaterials SA, Pelotas, Brazil), using the Flashforge Hunter DLP 3D printer (Flashforge 3D Technology Co. Ltd., Jinhua, China). The samples were designed in Ø9 × 2 mm and 65 mm × 10 mm × 3.3 mm dimensions in the Autodesk Meshmixer (Fusion 360 version, Autodesk Inc., San Rafael, CA, USA) software. The STL file was imported into FlashDLPrint software (Flashforge; 2.1.5 version; Zhejiang Flashforge 3D technology Co., LTD, Jinhua, China) and printed with a layer thickness of 100 µm and a vertical print orientation of 90 degrees. Then, the samples were washed in isopropyl alcohol for 5 min and post-cured for 10 min using a washing and curing machine (UW-01 Washing/Curing Machine; Creality 3D, Shenzhen, China). Following the process, the polish was done in a grinding and polishing machine with sandpapers of 80, 400, 600, and 1200 grit.

To evaluate the antimicrobial activity, the samples were previously sterilized in hydrogen peroxide and placed in 24-well plates (n = 9, Ø9 × 1 mm). In each well, 1500 µL of Brain Heart Infusion broth (BHI; Kasvi, Brazil; supplemented with yeast extract, glucose, and sucrose) was added, inoculated with the multispecies biofilm of *Candida albicans* (ATCC 10231), *Candida glabrata* (ATCC 2001), and *Streptococcus mutans* (ATCC 25175). The strains were previously standardized at $1 \times 10^6$ CFU/mL for *Candida spp*. and $1 \times 10^7$ CFU/mL for *S. mutans*. The plates were incubated at 37°C with stirring at 750 rpm for 90 min for biofilm adhesion. Then, the samples were washed in phosphate-buffered saline (PBS) twice to remove non-adherent cells, and 1500 µL of BHI was added. The plates were incubated again at 37°C with stirring at 750 rpm for 48 h for biofilm maturation. Half of the culture medium was replaced with a fresh medium after 24 h to offer nutrients.

After biofilm maturation, the samples were washed in PBS and transferred to tubes with 10 mL of Letheen Broth Base (Kasvi, São José dos Pinhais, Brazil) modified with 0.5% of Tween 80 (Polysorbate 80). The tubes were placed under ultrasonication (Altsonic Clean 9CA; ALT dental medical equipment Ltd., Sao Paulo, Brazil) for 20 min at 40 Hz and 200 W to detach the biofilm from the samples.

Aliquots of 25 µL were collected, serial dilutions were performed, and seeded in Petri plates in selective culture media: CHROMagar Candida (Difco Laboratories, Detroit, MI, EUA) for *C. albicans* and *C. glabrata*, and BHI agar (Kasvi) supplemented with 200 UI/mL nystatin for *S. mutans*. After incubation at 37°C for the growth of colonies, the colony-forming units per milliliter (CFU/mL) were counted (n = 9).

To evaluate the metabolic activity of the biofilm, aliquots of 100 µL were also collected from each tube, in triplicate, and transferred to 96-well plates (n = 9). The XTT Cell Viability Assay Kit (Uniscience, São Paulo, Brazil) was prepared according to the manufacturer's instructions, and 100 µL was added to each well. The plates were incubated at 37°C for 2 h in the dark. The absorbance reading was performed in a microplate spectrophotometer (Multiskan GO; Thermo Scientific, Waltham, MA, USA) at a wavelength of 492 nm.

Photomicrographs of the sample's surface (Ø9 × 2 mm) were obtained by Scanning Electron Microscopy (SEM; JSM-6610LV, JEOL, Tokyo, Japan) at 100, 500, 1000, and 10000 × magnifications. Surface roughness was evaluated using a 3D laser confocal microscope (LEXT 4000; Olympus, Tokyo, Japan). Three images were obtained for each sample (n = 10, Ø9 × 2 mm) with a resolution of 1024 × 1024 pixels and a magnification of 5 ×. The equipment software provided the roughness value (µm) of the three measurements, and the average roughness (Ra) was calculated.

Wettability was evaluated by the contact angle of water with the sample surface (n = 10, Ø9 × 2 mm) using a goniometer (CAM200, KSV Instruments Ltd., Helsinki, Finland). Three measurements were performed for each sample: 4 µL of distilled water was deposited at the surface, the drop stabilization was done for 60 s, and the measurement of contact angles (right and left) was carried out by the equipment software (CAM 200 Contact Angle Measurement System, KSV Instruments Ltd., Helsinki, Finland).

Three-point bending test was performed according to ISO 20795-1:2008, using a universal testing machine (EMIC DL 2000; São José dos Pinhais, São José dos Pinhais, Brazil). The samples (n = 10, 65 mm × 10 mm × 3.3 mm) were placed over the supports, positioned at a distance of 50 mm, and a load cell of 20 Kgf was applied in the center of the sample at a speed

of 5 mm/min until the fracture. Flexural strength (FS) was calculated by FS = $3WL/2bh^2$ (W: maximum load before fracture; L: span between supports; b: specimen width; h: specimen thickness). Elastic modulus (E) was calculated by E = $(P/d)$ $(L^3/[4bh^3])$ (P: load divided by displacement; d: slope in the elastic region of the tension/deformation curve).

Data distribution was verified using the Shapiro-Wilk test, and ANOVA and Tukey's post hoc tests were applied ($P < .05$) (IBM SPSS Statistics 20.0; IBM, Armonk, NY, USA). Pearson's Correlation Coefficient (r) was also used to evaluate the correlation among wettability, roughness, and antimicrobial activity.

## RESULTS

AgVO$_3$ powder showed vanadium nanowires with micrometer length and 150 nm in diameter approximately, and spherical silver nanoparticles on nanowires surface with 25 nm approximately (Fig. 1). Figure 2 shows that the incorporation of 10% of AgVO$_3$ into HT promoted major antimicrobial activity against *S. mutans* in relation to all groups ($P < .05$); however, this concentration (10%) favored *C. albicans* growth, with a statistical difference in relation to printed resin, HT 0% and 2.5% ($P < .05$). HT 10% apparently reduced

the CFU/mL of *C. glabrata* compared to printed resin and HT 2.5% ($P < .05$). However, the veracity of these results cannot be confirmed due to the high standard deviation in this group, which is explained by CFU/mL = 0 in some samples of *C. glabrata* and *S. mutans* in HT 10% (Supplementary Table 1). HT 5% reduced *S. mutans* count compared to printed resin ($P = .015$) but favored *C. albicans* growth compared to HT 0% ($P = .03$) (Fig. 2). The printed resin showed no differences in CFU/mL in relation to heat-cured resin (HT 0%).



**Fig. 1.** Photomicrograph of vanadate nanowires and silver nanoparticles of AgVO$_3$.
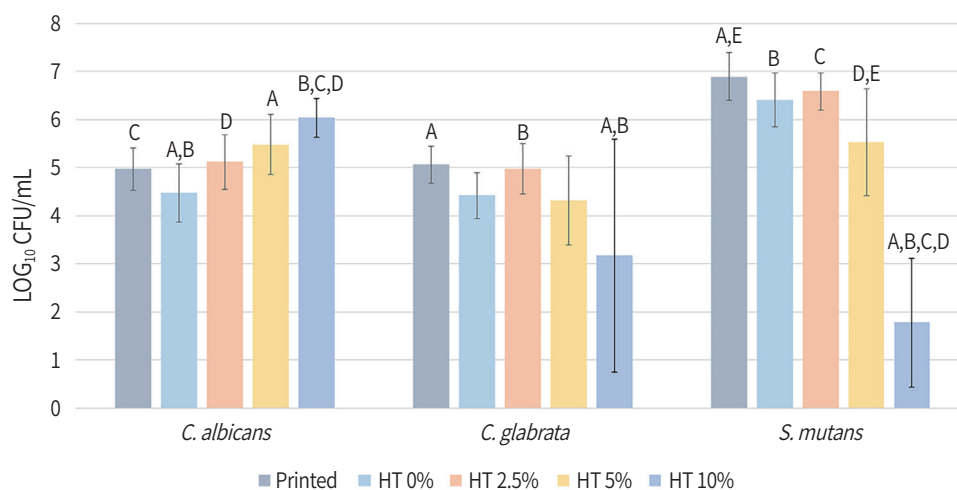


**Fig. 2.** Colony Forming Units per milliliter (CFU/mL) of multispecies biofilm of *Candida albicans*, *Candida glabrata*, and *Streptococcus mutans* formed for 48 hours in printed resin, conventional heat-cured resin (HT 0%), and antimicrobial resins incorporated with different concentrations of silver vanadate nanostructured decorated with silver nanoparticles (HT 2.5%, 5%, and 10%). Mean and standard deviation. ANOVA and Tukey's post hoc. [A,B,C,D,E] Equal letters indicate a statistical difference for each microorganism ($P < .05$).

However, the formed biofilm in HT 0% showed less metabolic activity than printed resin ($P$ = .023) and HT 10% of AgVO$_3$ ($P$ = .001) (Fig. 3).

Photomicrographs obtained by SEM display that the printed resin surface shows higher irregularity than HT 0% and 2.5%, both with surface smoothness. The HT 5% AgVO$_3$ had many porous on the surface, and the AgVO$_3$ was more visible on the HT 10% and 5% surfaces (Fig. 4). This was also observed in the micrographs obtained by laser confocal microscope, in which it is possible to notice that AgVO$_3$ particles formed clusters on the surface of the 10% group (Fig. 5), demonstrating that manual handling methods do not promote a good dispersion of the nanomaterial in the resin.

Despite these results, quantitatively there was no significant difference among the groups in surface roughness and wettability ($P$ > .05) (Fig. 5, Fig. 6). The type of resin and the incorporation of AgVO$_3$ did not influence these properties according to the methods used.
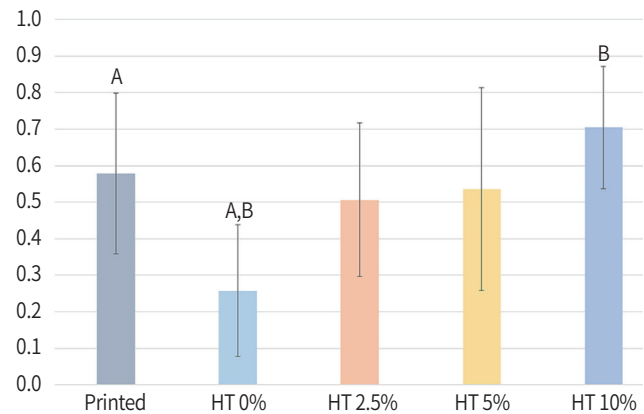


**Fig. 3.** Metabolic activity of multispecies biofilm of *Candida albicans*, *Candida glabrata*, and *Streptococcus mutans* formed for 48 hours in printed resin, conventional heat-cured resin (HT 0%), and antimicrobial resins incorporated with different concentrations of silver vanadate nanostructured decorated with silver nanoparticles (HT 2.5%, 5%, and 10%). Mean and standard deviation. ANOVA and Tukey's post hoc. [A,B] Equal letters indicate a statistical difference ($P$ < .05).
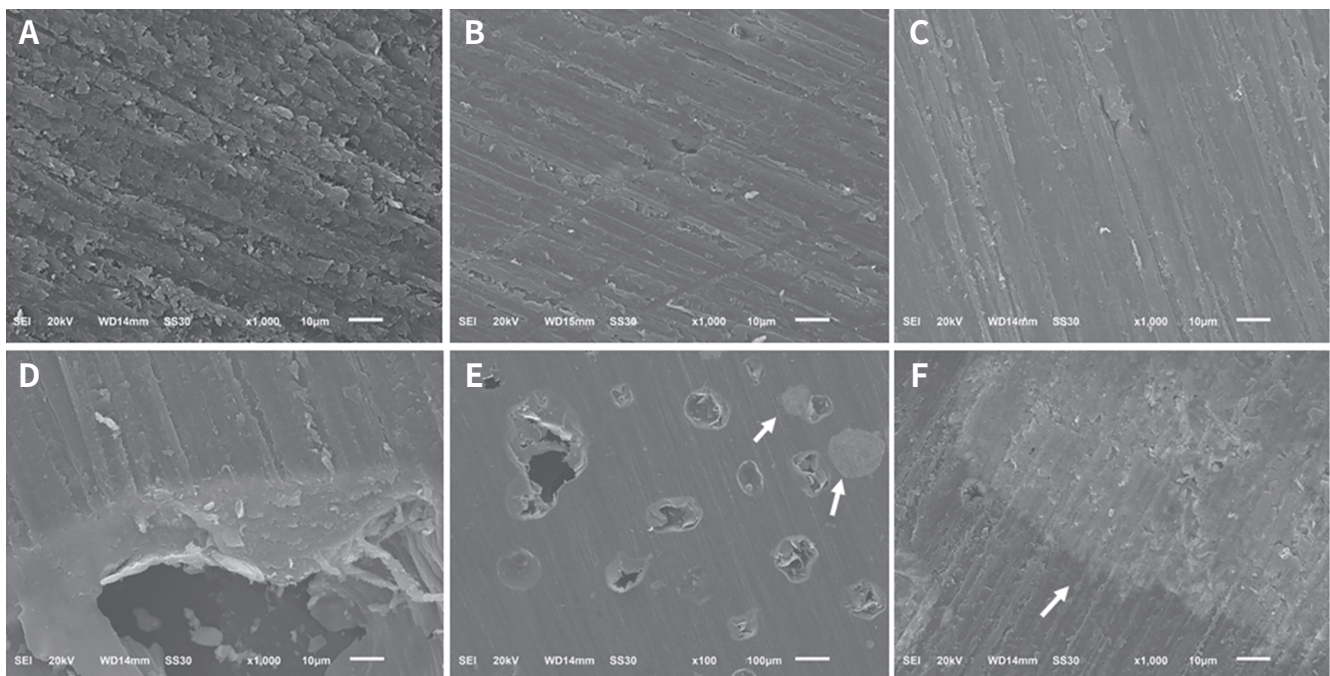


**Fig. 4.** Photomicrographs of printed resin, conventional heat-cured resin (HT 0%), and antimicrobial resins incorporated with different concentrations of silver vanadate nanostructured decorated with silver nanoparticles (HT 2.5%, 5%, and 10% AgVO$_3$). (A) Printed resin (× 1000 magnification), (B) HT 0% (× 1000 magnification), (C) HT 2.5% AgVO$_3$ (× 1000 magnification), (D) HT 5% AgVO$_3$ (× 1000 magnification), (E) HT 5% AgVO$_3$ (× 100 magnification), (F) HT 10% AgVO$_3$ (× 1000 magnification). Arrows indicate AgVO$_3$ particles.

**Fig. 5.** Average roughness and micrographs of printed resin, conventional heat-cured resin (HT 0%), and antimicrobial resins incorporated with different concentrations of silver vanadate nanostructured decorated with silver nanoparticles (HT 2.5%, 5%, and 10% AgVO$_3$) obtained in laser confocal microscope ($\times$ 5 magnification). (A) Roughness (mean and standard deviation), there was no statistical difference among the groups ($P$ > .05), (B) Printed, (C) HT 0%, (D) HT 2.5%, (E) HT 5%, (F) HT 10%. Arrows indicate AgVO$_3$ particles.
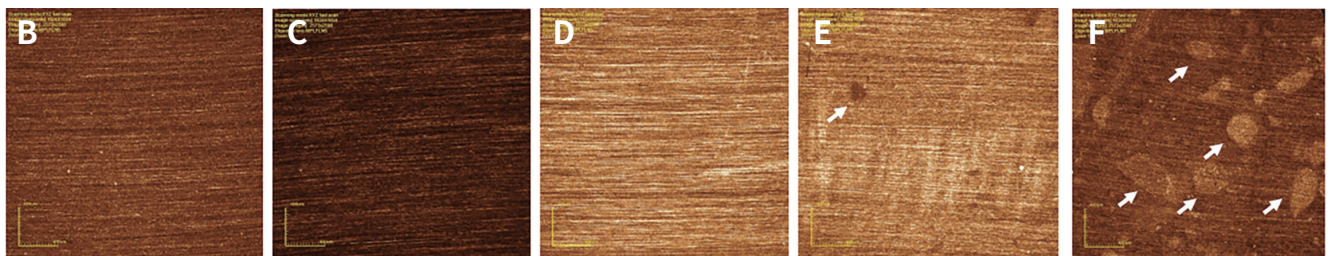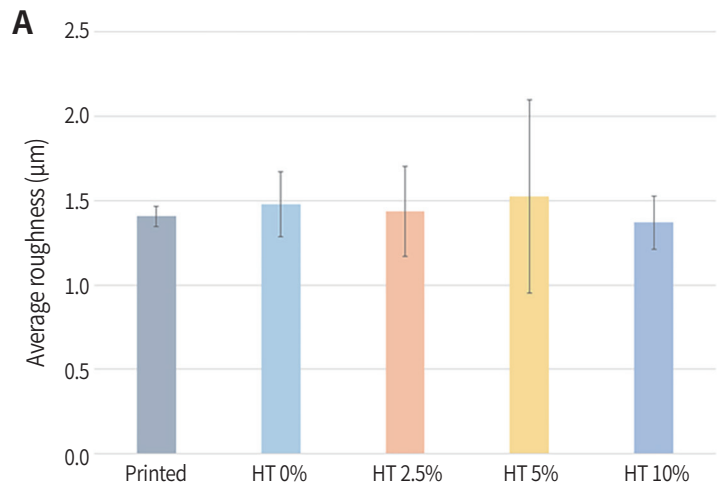


Pearson's correlation coefficient (r) showed that there is a strong and positive correlation between wettability and CFU/mL of *C. albicans* (r = 0.88). The correlation among the other variables (roughness, wettability, and CFU/mL) was considered weak (Table 1). The indices considered to indicate the strength of correlation between the variables were: > 0.70 is strong correlation; between 0.30 and 0.70 is moderate correlation; < 0.30 is weak correlation; equal to or close to 0 - no correlation. A positive correlation indicates that an increase in a variable causes an increase in the other, and a negative correlation indicates the opposite.

Heat-cured resin (HT 0%) showed higher flexural strength than printed and antimicrobial resins ($P$ < .05). The incorporation of AgVO$_3$ reduced this mechanical property. However, no differences were observed between the concentrations and printed resin ($P$ > .05) (Fig. 7A). The resins incorporated with AgVO$_3$ showed the highest elastic modulus, followed by HT 0% ($P$ < .05). The printed resin had the lowest elastic modulus among all groups ($P$ < .05) (Fig. 7B).



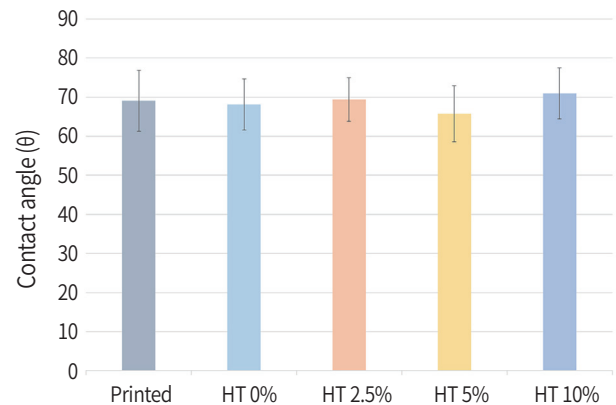**Fig. 6.** Contact angle between distilled water and surface of printed resin, conventional heat-cured resin (HT 0%), and antimicrobial resins incorporated with different concentrations of silver vanadate nanostructured decorated with silver nanoparticles (HT 2.5%, 5%, and 10% AgVO$_3$). Mean and standard deviation. ANOVA and Tukey's post hoc ($P$ < .05). There was no statistical difference among the groups.

**Table 1.** Pearson's correlation coefficient (r) between wettability, roughness, and Colony Forming Units per milliliter (CFU/mL) of multispecies biofilm of printed resin, conventional heat-cured resin (0%), and antimicrobial resins incorporated with nanostructured silver vanadate decorated with silver nanoparticles (AgVO$_3$)

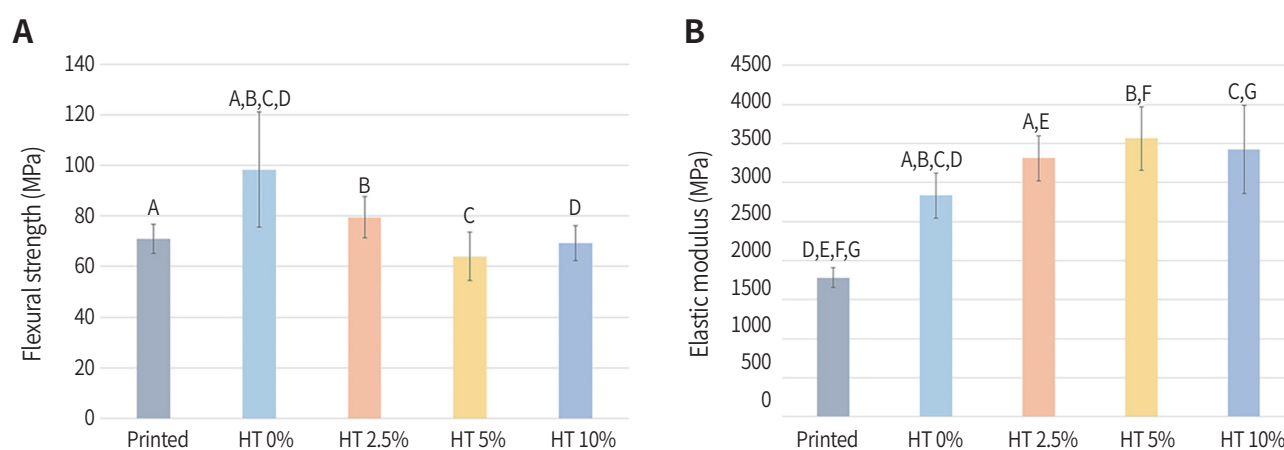| Correlation between variables | Pearson's coefficient (r) |
|---|---|
| Wettability × Roughness | 0.141 |
| Wettability × CFU/mL of *Candida albicans* | 0.88 |
| Wettability × CFU/mL of *Candida glabrata* | - 0.213 |
| Wettability × CFU/mL of *Streptococcus mutans* | - 0.191 |
| Roughness × CFU/mL of *Candida albicans* | - 0.135 |
| Roughness × CFU/mL of *Candida glabrata* | - 0.100 |
| Roughness × CFU/mL of *Streptococcus mutans* | - 0.008 |



**Fig. 7.** Mechanical properties of printed resin, conventional heat-cured resin (HT 0%), and antimicrobial resins incorporated with different concentrations of silver vanadate nanostructured decorated with silver nanoparticles (HT 2.5%, 5%, and 10% AgVO$_3$). Mean and standard deviation. ANOVA and Tukey's post hoc. (A) Flexural strength, (B) Elastic modulus. [A,B,C,D,E,F,G] Equal letters indicate a statistical difference ($P < .05$).

## DISCUSSION

The incorporation of AgVO$_3$ into heat-cured resin did not influence roughness or wettability, showed antimicrobial action against *S. mutans* in a multispecies biofilm (at a concentration of 10%), reduced flexural strength, and increased elastic modulus. Printed resin showed higher irregularity and metabolic activity of microorganisms and lower mechanical properties than heat-cured resin. Thus, the null hypothesis tested was partially accepted.

The antimicrobial action of AgVO$_3$ incorporated into acrylic resins against biofilms with a single species is proven,[22-24] demonstrating efficacy against *C. albicans* and *S. mutans* when incorporated into acrylic resins, alginate impression material, soft denture liners, and dental porcelains.[17-19,23,24] The antifungal action of AgVO$_3$ against the monospecies biofilm of *C. glabrata* has not yet been evaluated.

In this study, the amount of AgVO$_3$ incorporated into heat-cured resin was higher than the minimum inhibitory concentration (MIC) of the nanomaterial needed to inhibit the growth of *C. albicans* and *S. mutans*: 62.5 μg/mL and 250 μg/mL, respectively.[24] This conclusion was reached based on the ion release data presented by Castro *et al.*,[26] in which the amount of silver and vanadium ions released by the same concentrations of AgVO$_3$ used in this study exceeded the

MIC required for inhibition of these microorganisms. Thus, the increase in *C. albicans* CFU/mL is due to the multispecies biofilm model used.

In a multispecies biofilm, the co-aggregation, metabolic cooperation between species, quorum sensing, gene expression, and secretion of extracellular matrix make the response to antimicrobial agents more complex, but more similar to what occurs in the oral cavity.[25,27] Biofilm with *S. mutans* favors the growth of *Candida spp*. in experimental conditions, stimulating the co-aggregation and adhesion processes.[28] Pereira-Cenci *et al*.[29] also observed in a multispecies biofilm that *S. mutans* favored the growth of *C. albicans*, in line with the present study, whose growth of *C. albicans* increased in the HT 5% and 10% AgVO$_3$ groups. Therefore, it is likely that *S. mutans* aided in the growth of *C. albicans* and protected it from AgVO$_3$ action.

Despite the increase in *C. albicans*, HT 10% reduced the growth of *S. mutans* compared to all groups, and HT 5% decreased *S. mutans* CFU/mL compared to printed resin. Pores favor biofilm retention, and in spite of this, the group of 5% AgVO$_3$ showed an antimicrobial effect. Inhibition of these microorganisms by AgVO$_3$ can reduce mucosal inflammation and denture stomatitis, and potentially reduce caries in the remaining teeth of removable partial denture users.[25,29] *Candida glabrata* is frequently found on the palate mucosa and denture surface, and an imbalance can cause denture stomatitis together with *Candida albicans*.[29] *S. mutans* also composes the denture biofilm in association with *Candida spp*., in addition to being the primary etiologic agent of dental caries.[25,29]

The antimicrobial action of AgVO$_3$ comes from the release of silver and vanadium.[13-15] Silver nanoparticles act by inhibiting genes involved in biofilm formation (gtfB, gtfC, gtfD, and gbpB), in the protection of extracellular matrix (brpA, smu 360, and comDE), and in the survival of *S. mutans* in the oral environment (spaP and gyrA).[30] Against *C. glabrata*, its mechanism of action involves changes in the yeast's outer layer, in fatty acid composition, and blocking ATP synthesis.[31]

A limitation of this study was the high standard deviation observed in the HT 10% group, which oc-

curred because some samples had CFU = 0 for *C. glabrata* and *S. mutans*. Data and statistical tests were reviewed, but due to the high standard deviation for *C. glabrata*, it is not possible to state that HT 10% was effective against this microorganism.

The assessment of biofilm metabolic activity is complementary to that of CFU/mL because, although there is inhibition in the growth of some species, the remaining biofilm can maintain metabolically active mitochondrial function.[28] In this study, HT 10% and printed resin had more metabolically active cells than HT 0%. The increase in *C. albicans* CFU/mL in HT 10% justifies the result of the metabolic activity. For printed resin, the higher irregularity observed on their surface by SEM (Fig. 4) can favor the retention of microorganisms.

Sample disinfection for microbiological analysis was performed using hydrogen peroxide because it is a low-temperature sterilization method since high temperatures can promote damage to antimicrobials.[32,33] This gas sterilization is safe and widely used in medical devices;[34,35] however, it causes an increase in surface hydrophilicity, providing greater cell adhesion.[36-38] Despite this finding, hydrogen peroxide does not seem to have influenced this study's results since the antimicrobial effect observed is due to the nanomaterial properties, and wettability was evaluated in samples without sterilization.

Hydrophilicity and surface roughness also directly influence the microorganisms' adhesion.[23,25,29] In this study, no statistical difference was observed among the groups in wettability or roughness, indicating that the sample's manual polishing protocol made it possible to obtain a smooth surface for most groups. However, the pores observed on HT 5% surface (Fig. 4) can have been formed during the sample's polishing since the sandpaper could have displaced AgVO$_3$ particles agglomerated on the surface. These pores also caused a high standard deviation in the evaluation of roughness in this group.

Differences in the printed resin and HT 0% surfaces were also observed by Gad *et al*.,[39] in which the printed resin showed more irregularity, pores, and deep valleys in SEM analysis. But the printed resin roughness was lower than the heat-cured resin, which was attributed to the lower layer thickness (50 μm). The

authors also observed that 90 degrees of print orientation resulted in higher roughness.[39]

In this study, the samples were printed with a layer thickness of 100 μm and a print orientation of 90 degrees, based on studies in which this orientation showed less roughness and biofilm accumulation[40] and this layer thickness showed better accuracy than 50 μm,[41] demonstrating that there is still no consensus in the literature regarding the ideal layer thickness and print orientation.[2]

Pearson's correlation coefficient indicated a positive and strong correlation between wettability and CFU/mL of *C. albicans*; thus, the greater the surface wettability, the greater *C. albicans* adhesion. But as there was no significant difference in wettability among the groups, the results in CFU/mL were probably due to the relationship between the species used in this biofilm model.

A fracture of the upper denture in the midline usually occurs due to constant flexion induced by masticatory forces. A denture base with satisfactory flexural strength and elastic modulus, which reflects the material's stiffness, is more resistant to fractures and permanent deformations.[42-44] When a nanomaterial is incorporated into PMMA, its final mechanical properties depend on the particles' incorporated concentration, shape, size, and interaction with the polymeric matrix.[42]

Flexural strength reduction in resins incorporated with $AgVO_3$ can be expected since pores and the nanomaterial agglomeration in the polymer matrix cause a stress concentration area. Castro *et al*.[23] observed a flexural strength reduction in resins incorporated with $AgVO_3$, which is due to the limited dispersion of the nanomaterial in the matrix, which is inherent to the manual incorporation method. The method was also used in this study and chosen for its ease of access and low processing cost. $AgVO_3$ is an inorganic compound of a hydrophilic nature incapable of chemically bonding to the hydrophobic polymeric chain.[23] Nanomaterial functionalization and particle coating with substances that form bonds with the resin may be an option for improving dispersion and mechanical resistance.

In this study, printed resin showed lower flexural strength than heat-cured resin, according to results observed in other studies.[39,45-47] The 3D-printing resin shows a lower degree of double bond conversion than conventional resins; the weak bond between layers and the need for post-curing reduce the material's mechanical performance.[45,47] Printing orientation also influenced the results of this study, as samples printed horizontally (0 degrees) showed better flexural strength than samples printed vertically (90 degrees).[39,40,46]

Although printed and incorporated with $AgVO_3$ resins showed lower flexural strength than HT 0%, they meet the ISO 20795-1:2013 requirement, in which the minimum flexural strength of denture base polymers must be 65 MPa.[45,47]

A possible explanation for the increase in elastic modulus from the incorporation of $AgVO_3$ into heat-cured resin is that the nanoparticles distributed in the matrix minimize the polymer chain movement effect, which increases the material's rigidity.[42,43,48] Thus, the modified resin can clinically resist permanent deformation caused by masticatory forces.[43] However, when not well distributed, the nanoparticles form clusters and some areas of the polymer is left unreinforced without the immobilization effect.[42] Despite the elastic modulus increase, cracks can propagate through these areas,[42] which probably led to the low flexural strength of the modified material. Conventional heat-cured resins and those incorporated with $AgVO_3$ showed an elastic modulus above that recommended by the American Dental Association (2000 MPa).[42,43] The printed resin did not reach the recommended minimum value.

The results of this study must be interpreted with caution before clinical applicability. The $AgVO_3$ incorporated into heat-cured resin at the same concentrations evaluated in the present study demonstrated a cytotoxic effect for mouse fibroblasts (L929 cells).[26] Its biocompatibility with gingival and palate cells must be verified.

In addition, this study has some limitations, such as (1) a small sample size, which caused a high standard deviation in CFU/mL and roughness evaluation; (2) the multispecies biofilm used does not properly simulate the oral cavity biofilm; (3) the polishing protocol may have stripped nanoparticles from the HT 5% surface, causing pores; (4) tests were performed on

specimens that do not resemble a denture base; (5) the printed resin has a different composition, which made it difficult to compare it with the modified heat-cured resin.

The results of this study on printed resin indicate that it has a greater porosity than heat-cured resin. Further investigations about their porosity, water absorption, surface characteristics with different layer thicknesses and print orientations, mechanical performance, and incorporation of antimicrobials such as $AgVO_3$ to reduce biofilm accumulation could be carried out.

Furthermore, the incorporation of $AgVO_3$ into PMMA has the potential to reduce the adhesion of *S. mutans* to the base of the prosthesis, which contributes to the general health of denture-wearing patients.

## CONCLUSION

It was concluded that the incorporation of $AgVO_3$ into heat-cured resin showed antimicrobial action against *Streptococcus mutans* (at a 10% concentration), reduced flexural strength, increased elastic modulus, and did not influence surface roughness or wettability. Printed resin for denture bases showed higher irregularities, a metabolically active biofilm, lower flexural strength and elastic modulus than heat-cured resin.

## REFERENCES

1. da Silva Barboza A, Fang LK, Ribeiro JS, Cuevas-Suárez CE, Moraes RR, Lund RG. Physicomechanical, optical, and antifungal properties of polymethyl methacrylate modified with metal methacrylate monomers. J Prosthet Dent 2021;125:706.e1-6.
2. Vilela Teixeira AB, Dos Reis AC. Influence of parameters and characteristics of complete denture bases fabricated by 3D printing on evaluated properties: a scoping review. Int J Prosthodont 2021 May 17. (Epub ahead of print)
3. Totu EE, Nechifor AC, Nechifor G, Aboul-Enein HY, Cristache CM. Poly(methyl methacrylate) with TiO2 nanoparticles inclusion for stereolitographic complete denture manufacturing - the fututre in dental care for elderly edentulous patients? J Dent 2017;59: 68-77.
4. AlMojel N, AbdulAzees PA, Lamb EM, Amaechi BT. Determining growth inhibition of Candida albicans biofilm on denture materials after application of an organoselenium-containing dental sealant. J Prosthet Dent 2023;129:205-12.
5. Lee HL, Wang RS, Hsu YC, Chuang CC, Chan HR, Chiu HC, Wang YB, Chen KY, Fu E. Antifungal effect of tissue conditioners containing poly(acryloyloxyethyl-trimethyl ammonium chloride)-grafted chitosan on Candida albicans growth in vitro. J Dent Sci 2018;13: 160-6.
6. Iqbal Z, Zafar MS. Role of antifungal medicaments added to tissue conditioners: A systematic review. J Prosthodont Res 2016;60:231-9.
7. Muttagi S, Subramanya JK. Effect of incorporating seed oils on the antifungal property, surface roughness, wettability, weight change, and glucose sorption of a soft liner. J Prosthet Dent 2017;117:178-85.
8. Hotta J, Garlet GP, Cestari TM, Lima JFM, Porto VC, Urban VM, Neppelenbroek KH. In vivo biocompatibility of an interim denture resilient liner containing antifungal drugs. J Prosthet Dent 2019;121:135-42.
9. Morse DJ, Wilson MJ, Wei X, Bradshaw DJ, Lewis MAO, Williams DW. Modulation of Candida albicans virulence in in vitro biofilms by oral bacteria. Lett Appl Microbiol 2019;68:337-43.
10. Altinci P, Mutluay M, Söderling E, Tezvergil-Mutluay A. Antimicrobial efficacy and mechanical properties of BAC-modified hard and soft denture liners. Odontology 2018;106:83-9.
11. Marra J, Paleari AG, Rodriguez LS, Leite AR, Pero AC, Compagnoni MA. Effect of an acrylic resin combined with an antimicrobial polymer on biofilm formation. J Appl Oral Sci 2012;20:643-8.
12. Deyab MH, Awady BE, Bakir NG. Is immersion in mint oil or apple vinegar solution a valid antifungal approach for acrylic soft liners? Future Dent J 2018;4: 302-7.
13. Holtz RD, Lima BA, Souza Filho AG, Brocchi M, Alves OL. Nanostructured silver vanadate as a promising antibacterial additive to water-based paints. Nanomedicine 2012;8:935-40.
14. de Campos MR, Botelho AL, Dos Reis AC. Nanostructured silver vanadate decorated with silver particles and their applicability in dental materials: A scope re-

view. Heliyon 2021;7:e07168.

15. Teixeira ABV, Moreira NCS, Takahashi CS, Schiavon MA, Alves OL, Reis AC. Cytotoxic and genotoxic effects in human gingival fibroblast and ions release of endodontic sealers incorporated with nanostructured silver vanadate. J Biomed Mater Res B Appl Biomater 2021;109:1380-8.

16. de Castro DT, Teixeira ABV, do Nascimento C, Alves OL, de Souza Santos E, Agnelli JAM, Dos Reis AC. Comparison of oral microbiome profile of polymers modified with silver and vanadium base nanomaterial by next-generation sequencing. Odontology 2021;109: 605-14.

17. Vidal CL, Ferreira I, Ferreira PS, Valente MLC, Teixeira ABV, Reis AC. Incorporation of hybrid nanomaterial in dental porcelains: antimicrobial, chemical, and mechanical properties. Antibiotics 2021;10:98.

18. de Castro DT, Kreve S, Oliveira VC, Alves OL, Dos Reis AC. Development of an impression material with antimicrobial properties for dental application. J Prosthodont 2019;28:906-12.

19. Kreve S, Oliveira VC, Bachmann L, Alves OL, Reis ACD. Influence of AgVO3 incorporation on antimicrobial properties, hardness, roughness and adhesion of a soft denture liner. Sci Rep 2019;9:11889.

20. Vilela Teixeira AB, Larissa Vidal C, Albiasetti T, Tornavoi de Castro D, Cândido Dos Reis A. Influence of adding nanoparticles of silver vanadate on antibacterial effect and physicochemical properties of endodontic sealers. Iran Endod J 2019;14:7-13.

21. Vilela Teixeira AB, de Carvalho Honorato Silva C, Alves OL, Cândido Dos Reis A. Endodontic sealers modified with silver vanadate: antibacterial, compositional, and setting time evaluation. Biomed Res Int 2019; 2019:4676354.

22. de Castro DT, Valente ML, Agnelli JA, Lovato da Silva CH, Watanabe E, Siqueira RL, Alves OL, Holtz RD, dos Reis AC. In vitro study of the antibacterial properties and impact strength of dental acrylic resins modified with a nanomaterial. J Prosthet Dent 2016;115:238-46.

23. de Castro DT, Valente ML, da Silva CH, Watanabe E, Siqueira RL, Schiavon MA, Alves OL, Dos Reis AC. Evaluation of antibiofilm and mechanical properties of new nanocomposites based on acrylic resins and silver vanadate nanoparticles. Arch Oral Biol 2016;67:46-53.

24. Castro DT, Holtz RD, Alves OL, Watanabe E, Valente ML, Silva CH, Reis AC. Development of a novel resin with antimicrobial properties for dental application. J Appl Oral Sci 2014;22:442-9.

25. Lopes Vasconcelos GL, Curylofo PA, Targa Coimbra FC, de Cássia Oliveira V, Macedo AP, de Freitas Oliveira Paranhos H, Pagnano VO. In vitro antimicrobial activity of effervescent denture tablets on the components of removable partial dentures. Int J Prosthodont 2020; 33:315-20.

26. de Castro DT, Valente MLDC, Aires CP, Alves OL, Dos Reis AC. Elemental ion release and cytotoxicity of antimicrobial acrylic resins incorporated with nanomaterial. Gerodontology 2017;34:320-25.

27. Marino PJ, Wise MP, Smith A, Marchesi JR, Riggio MP, Lewis MAO, Williams DW. Community analysis of dental plaque and endotracheal tube biofilms from mechanically ventilated patients. J Crit Care 2017;39:149-55.

28. Quishida CC, Mima EG, Dovigo LN, Jorge JH, Bagnato VS, Pavarina AC. Photodynamic inactivation of a multispecies biofilm using Photodithazine(®) and LED light after one and three successive applications. Lasers Med Sci 2015;30:2303-12.

29. Pereira-Cenci T, Deng DM, Kraneveld EA, Manders EM, Del Bel Cury AA, Ten Cate JM, Crielaard W. The effect of Streptococcus mutans and Candida glabrata on Candida albicans biofilms formed on different surfaces. Arch Oral Biol 2008;53:755-64.

30. Al-Ansari MM, Al-Dahmash ND, Ranjitsingh AJA. Synthesis of silver nanoparticles using gum Arabic: Evaluation of its inhibitory action on Streptococcus mutans causing dental caries and endocarditis. J Infect Public Health 2021;14:324-30.

31. Darwish RM, AlKawareek MY, Bulatova NR, Alkilany AM. Silver nanoparticles, a promising treatment against clinically important fluconazole-resistant Candida glabrata. Lett Appl Microbiol 2021;73:718-24.

32. Lee JH, El-Fiqi A, Jo JK, Kim DA, Kim SC, Jun SK, Kim HW, Lee HH. Development of long-term antimicrobial poly(methyl methacrylate) by incorporating mesoporous silica nanocarriers. Dent Mater 2016;32:1564-74.

33. Kim KI, Kim DA, Patel KD, Shin US, Kim HW, Lee JH, Lee HH. Carbon nanotube incorporation in PMMA to

prevent microbial adhesion. Sci Rep 2019;9:4921.

34. Noda M, Sakai Y, Sakaguchi Y, Hayashi N. Evaluation of low-temperature sterilization using hydrogen peroxide gas containing peracetic acid. Biocontrol Sci 2020; 25:185-91.

35. McEvoy B, Rowan NJ. Terminal sterilization of medical devices using vaporized hydrogen peroxide: a review of current methods and emerging opportunities. J Appl Microbiol 2019;127:1403-20.

36. de Sousa-Lima RX, de Lima JFM, Silva de Azevedo LJ, de Freitas Chaves LV, Alonso RCB, Borges BCD. Surface morphological and physical characterizations of glass ionomer cements after sterilization processes. Microsc Res Tech 2018;81:1208-13.

37. Tong W, Tran PA, Turnley AM, Aramesh M, Prawer S, Brandt M, Fox K. The influence of sterilization on nitrogen-included ultrananocrystalline diamond for biomedical applications. Mater Sci Eng C Mater Biol Appl 2016;61:324-32.

38. Junkar I, Kulkarni M, Drašler B, Rugelj N, Mazare A, Flašker A, Drobne D, Humpolíček P, Resnik M, Schmuki P, Mozetič M, Iglič A. Influence of various sterilization procedures on TiO2 nanotubes used for biomedical devices. Bioelectrochemistry 2016;109:79-86.

39. Gad MM, Fouda SM, Abualsaud R, Alshahrani FA, Al-Thobity AM, Khan SQ, Akhtar S, Ateeq IS, Helal MA, Al-Harbi FA. Strength and surface properties of a 3D-printed denture base polymer. J Prosthodont 2022;31:412-8.

40. Shim JS, Kim JE, Jeong SH, Choi YJ, Ryu JJ. Printing accuracy, mechanical properties, surface characteristics, and microbial adhesion of 3D-printed resins with various printing orientations. J Prosthet Dent 2020;124:468-75.

41. You SM, You SG, Kang SY, Bae SY, Kim JH. Evaluation of the accuracy (trueness and precision) of a maxillary trial denture according to the layer thickness: An in vitro study. J Prosthet Dent 2021;125:139-45.

42. Alzayyat ST, Almutiri GA, Aljandan JK, Algarzai RM, Khan SQ, Akhtar S, Ateeq IS, Gad MM. Effects of SiO2 incorporation on the flexural properties of a denture base resin: an in vitro study. Eur J Dent 2022;16:188-94.

43. Gad MM, Ali MS, Al-Thobity AM, Al-Dulaijan YA, Zayat ME, Emam AM, Akhtar S, Khan SQ, Al-Harbi FA, Fouda SM. Polymethylmethacrylate incorporating nanodi-

amonds for denture repair: in vitro study on the mechanical properties. Eur J Dent 2022;16:286-95.

44. Ajaj-Alkordy NM, Alsaadi MH. Elastic modulus and flexural strength comparisons of high-impact and traditional denture base acrylic resins. Saudi Dent J 2014;26:15-8.

45. Perea-Lowery L, Gibreel M, Vallittu PK, Lassila LV. 3D-printed vs. heat-polymerizing and autopolymerizing denture base acrylic resins. Mater (Basel) 2021; 14:5781.

46. Srinivasan M, Kamnoedboon P, McKenna G, Angst L, Schimmel M, Özcan M, Müller F. CAD-CAM removable complete dentures: A systematic review and meta-analysis of trueness of fit, biocompatibility, mechanical properties, surface characteristics, color stability, time-cost analysis, clinical and patient-reported outcomes. J Dent 2021;113:103777.

47. Prpić V, Schauperl Z, Čatić A, Dulčić N, Čimić S. Comparison of mechanical properties of 3D-printed, CAD/CAM, and conventional denture base materials. J Prosthodont 2020;29:524-8.

48. Choi JJE, Uy CE, Ramani RS, Waddell JN. Evaluation of surface roughness, hardness and elastic modulus of nanoparticle containing light-polymerized denture glaze materials. J Mech Behav Biomed Mater 2020; 103:103601.